Dual-Band Printed Monopole Antenna Design

Hassan A. Ragheb, Shady Abd El-Aal, Afaf Saad, and Ahmed Zaalouk

Department of Electrical Engineering
The British University in Egypt, El Sherouk City, Misr-Ismaillia Road, Egypt
Hassan.Ragheb@bue.edu.eg

Abstract **─** Design procedure of a high gain dual-band printed monopole antenna, resonating at 2.4 GHz and 5.5 GHz, is presented. The proposed design meets the specifications required by WI-FI, WIMAX and radio frequency identification (RFID) reader applications. Our design utilizes Rogers RT/Duroid 5880(tm) substrate, and the major radiation element is an annular circular patch shape. The design was improved by adding a face-to-face fork shape metal inside the annular circular patch. The antenna feed consists of a microstrip line and a slotted transformer section for matching purpose. A prototype of the proposed antenna was fabricated and the measurements of the return loss and antenna radiation pattern were performed. The comparison between the results obtained from the simulation and the measurements showed an excellent agreement.

I. INTRODUCTION

Recent advances in Radio Frequency Identification (RFID) led to the invention of new antennas for both the tag and the reader. This is due to the increasing number of applications that can employ RFID. The RFID reader may have a high gain and multiband antenna to read the tag information correctly. Dual band microstrip antennas became suitable candidate for RFID and modern communication applications. Accordingly, extensive research was published for inventing efficient dual band antennas.

In general, many techniques have been used for designing dual band microstrip antennas. Among them are etching of slots from the radiating element [1]. Hamad [2] used slot etching to design two different dual-band rectangular microstrip antennas for the RFID application. The first antenna resonates at 2.46 GHz and 5.78 GHz and operates at frequency bands (2.4-2.5 GHz) and (5.6-5.8 GHz). The second antenna resonates at 2.47 GHz and 5.8 GHz while the bandwidth is from 2.4 to 2.5 GHz and from 5.8 to 6 GHz. A tapered structure technique fed by coplanar waveguide [3] had also been investigated. The integration of metamaterials with antennas [4] was also employed for dual band design. Rafiqul et al. [5] designed a dual-band microstrip patch antenna using metamaterial for mobile GSM and WiMax application. An array of five split ring resonators (SRRs) unit cells was inserted under the patch. The antenna resonates at 1.8 GHz for mobile GSM and 2.4 GHz for WIMAX applications. Multilayered structure had been proposed for the design of dual band antenna. Dual-band operation of a single-feed composite cavity-backed four-arm curl antenna was presented in [6]. Dual-band operation was achieved with the presence of the asymmetrical arm structure. A pair of vacant-quarter printed rings was used in the feed structure to produce a good circular polarization (CP) at both bands. Another technique, known as the *defected ground plane technique*, modifies the ground plane instead of the radiating patch to meet the multiband requirements [7,8]. Monopole structure has also been used for dual band design. Panda and Kshetrimayum [9] designed a simple microstrip that fed folded strip monopole antenna with a protruding stub in the ground plane for the application in WLAN and RFID. The antenna supports two resonances at 2.4 GHz and 5.81 GHz, which are the center frequencies of WLAN and RFID, respectively. The design of a simple and compact dual frequency monopole antenna for Personal Communication System (PCS) and Bluetooth applications was presented in [10]. The first operating frequency was achieved from a traditional monopole antenna structure for the frequency of 1.9 GHz for PCS application, while the second operating frequency is obtained from two spur line structures etched on the traditional monopole antenna structure for the frequency of 2.4 GHz for the Bluetooth application. A novel printed slot antenna with circular polarization characteristics using an L-shaped slot in the ground plane and an L-shaped radiating stub with a pair of Γ-shaped slits was presented in [11]. The operating frequencies of the proposed antenna are 5.2/5.8 GHz, which covers WLAN system, 5.5 GHz for WiMAX system, and 4 GHz for C-Band system. Compact array of printed dipole antennas loaded with reactive elements was presented in [12]. The design was successfully working at 0.9 GHz and 1.6 Ghz.

This paper aims at designing a high gain dual-band microstrip antenna. The first step in the design started with calculating the radius of the circular patch antenna operating at 2.4 GHz. In order to have another resonance

Submitted On: January 8, 2020
Accepted On: October 4, 2020
https://doi.org/10.47037/2020.ACES.J.351009

at 5.5 GHz the circular patch is slotted to produce an annular ring. Finally to enhance the antenna gain the design is modified by adding face-to-face fork-shaped metals inside the annular ring. The final design is fabricated using Rogers RT/duroid 5880(tm) substrate. Measurements of S_{11}, antenna radiation pattern and gain are carried out. Measured results showed excellent agreement with the simulation results

II. DESIGN PROCEDURE

As an initial design, a circular patch antenna radiating at 2.4 GHz was considered, as shown in Fig. 1. The resonance frequency of a circular patch microstrip antenna is given by [13]:

$$(f_{r\,mn0}) = \frac{x'_{mn}}{\sqrt{\mu\epsilon}2\pi R}, \quad (1)$$

where x'_{mn} refers to zeroes of the Bessel function derivative and R is the radius of the circular patch. The dominant mode is TM_{110}, corresponding to $x'_{11} = 1.8412$. Thus,

$$(f_{r\,110}) = \frac{1.8412 v_0}{2\pi R\sqrt{\epsilon_r}}, \quad (2)$$

where $v_0 = \frac{1}{\sqrt{\epsilon_0 \mu_0}} = 3 \times 10^8 \ \ m/s$ and ϵ_r is the relative permittivity of the substrate. Equation (1) does not take the fringing effect into consideration. This effect makes the patch appears larger than the real size, so the effective radius R_e after the fringing effect is as follows:

$$R_e = R\{1 + \frac{2h}{\pi R \epsilon_r}\left[\ln\left(\frac{\pi R}{2h}\right) + 1.7726\right]\}^{0.5}, \quad (3)$$

where h is the substrate height. Therefore,

$$(f_{r\,110}) = \frac{1.8412 v_0}{2\pi R_e \sqrt{\epsilon_r}}. \quad (4)$$

If one uses $f_{r\,110} = 2.4\,GHz$ then the radius of the circular patch as 2.1 cm considering $h\ =\ 0.157\ cm$ and $\epsilon_r = 2.2$ can be obtained. The feed line of this patch is also designed using the microstrip transmission line formula, namely, [14]:

$$\frac{w}{h} = \frac{2}{\pi}\left\{B - 1 - \ln(2B-1) + \frac{\epsilon_r - 1}{2\epsilon_r}\left[\ln(B-1) + 0.39 - \frac{0.61}{\epsilon_r}\right]\right\}$$

where $B = \frac{377\pi}{2Z_0\sqrt{\epsilon_r}}$, $Z_0 = 50\Omega$. (5)

Upon using (5), the feed line width is found to be $0.306\ cm$. In order to match the circular patch to 50Ω feed line, a wide transmission line transformer is inserted between the patch and the line. The wider line is then slotted in order to have proper matching. This is done employing HFSS parametric study. The length of the wide transmission line is initially taken as 6 cm while its width is 3.5 cm. The slot dimensions are $3\ cm \times 1 cm$. The initial design dimensions are used in HFSS simulation package in which the patch and feed layout are illustrated in Fig. 1. The ground plane height is considered as a parameter, and the reflection coefficient S_{11} is calculated at different values of the ground plan height. The best result found at a ground plane height is 6.5 cm. The resulting reflection coefficient S_{11} corresponding to the initial design is illustrated in Fig. 2. As shown in Fig. 2, S_{11} corresponding to the initial design resonates at 2.4 GHz, 4.8 GHz, and 5.6 GHz.

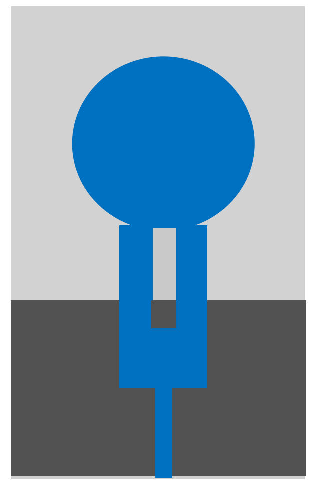

Fig. 1. Initial design of the monopole antenna.

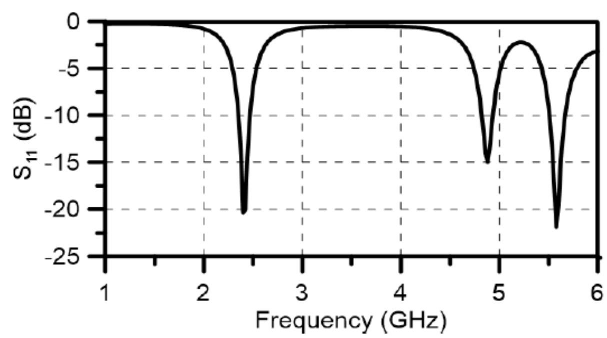

Fig. 2. S_{11} at different frequencies.

In order to eliminate the resonance at 4.8 GHz, the matching section dimensions are considered as a parameter in HFSS. A parametric study is employed to obtain the pre-specified resonance frequencies and to improve S_{11}. The optimum values obtained are found to be $5\ cm \times 2.5\ cm$ for the outer dimensions of the rectangle and $4\ cm \times 1\ cm$ for the inner dimensions of the rectangle. The antenna resonates at 2.4 GHz and 5.5 GHz as shown in Fig. 3. There is an improvement in S_{11} in the last result, but the antenna gain still needs to be enhanced.

Thus, an improved design suggests creating a slot in the circular patch as shown in Fig. 4. The inner and outer radii of the annular ring are then considered as parameters in HFSS simulation package. The optimum value of the inner radius is 2.5 cm, while the outer radius of the annular ring is 3.5 cm. In such a case, the antenna has resonance at 2.4 GHz and 5.5 GHz with higher gain as desired; however, there is an undesired small dip at

4.8 as shown in Fig. 5.

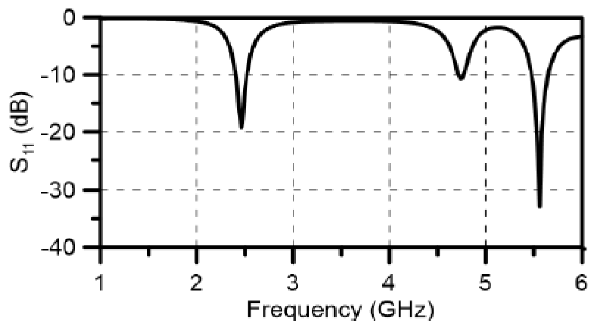

Fig. 3. S_{11} at different frequencies.

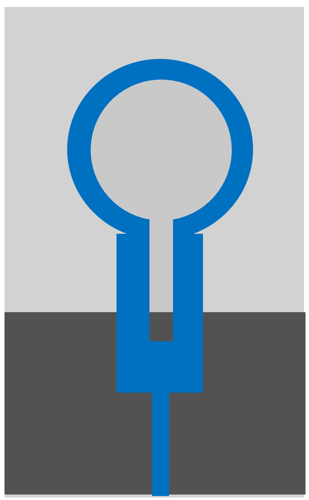

Fig. 4. Improved design of the monopole antenna.

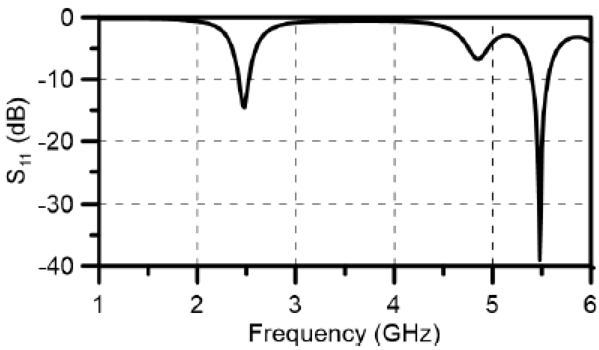

Fig. 5. S_{11} at different frequencies.

The result achieved the desirable S_{11}, the bandwidth at the two resonance frequencies and the gain need to be increased. Therefore, the antenna design is modified by adding face-to-face fork-shaped metals inside the annular ring as shown in Fig. 6. The radii of the fork shape resonators were considered as parameters in the HFSS simulation package to obtain optimal dimensions. Finally, to obtain an optimized antenna parameter, which gives high gain wide bandwidth, and the dual resonance, 183 trials (by changing some parameters and fixing the others) were performed. The final design dimensions are illustrated in Table 1, produce an antenna efficiency of 86%.

Table 1: Optimized antenna parameters

Label	Value (cm)	Label	Value (cm)
L_1	16	w_3	4.1
L_2	7.98	w_4	0.306
L_3	5	a_1	3.1
L_4	4	a_2	2.1
L_5	3.2	a_3	1.42
w_1	10	a_4	0.92
w_2	0.51	h	0.157

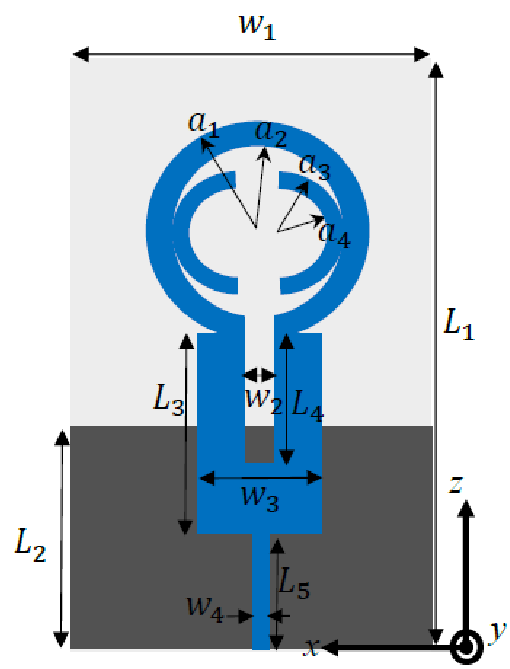

Fig. 6. Final antenna design.

III. FABRICATION AND FINAL SIMULATION

The dimensions given in Table 1 are used to fabricate the antenna using Rogers RT/duroid 5880(tm) substrate. The antenna fabrication and measurements of S_{11} were performed at the National Telecom Institute (NTI) in Cairo, Egypt. The Vector Network Analyzer shown in Fig. 7 was utilized to measure S_{11}. Meanwhile, by employing the above dimensions in the simulation package, the theoretical results for S_{11} were obtained.

The measured and simulated results of the S_{11} in the frequency range 0-6 GHz are illustrated in Fig. 8. Thus, an excellent agreement between the measured loss and the simulated return loss S_{11} is obtained. Figure 8 shows that there are only two resonances at 2.4 GHz and 5.5 GHz. In addition, the antenna gain is maximized.

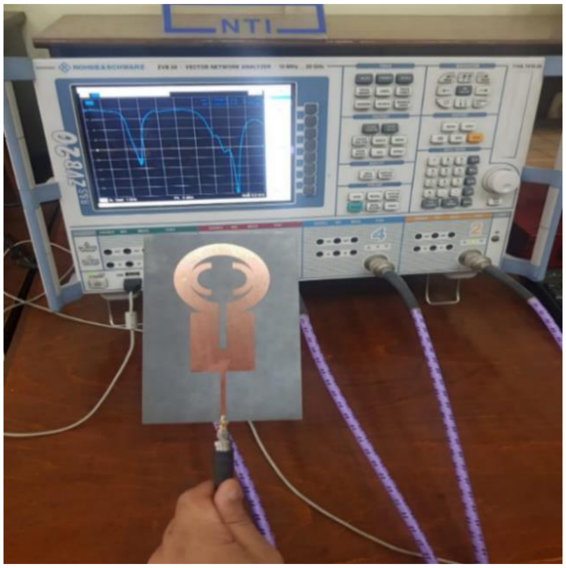

Fig. 7. Fabricated antenna.

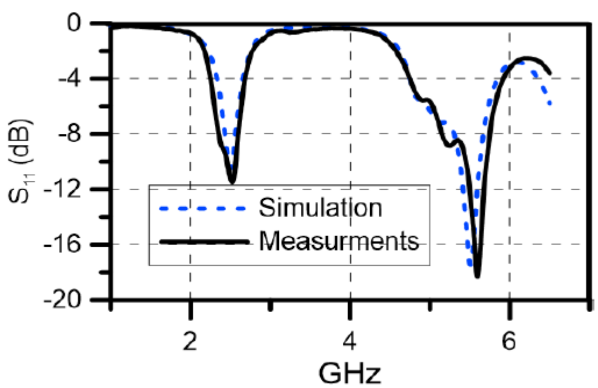

Fig. 8. Measured and simulated S_{11} of the proposed antenna.

The designed antenna's radiation pattern and gain are measured using the facilities at the Military Excellence Center as shown in Fig. 9.

The maximum gain at different values of frequency is measured and the results are illustrated in Fig. 10. As shown in Fig. 10, the maximum gain was shown at 2.5 and 5.5 GHz to be (6.47 dB) and (8.52 dB), respectively. The comparison of the antenna gain between our proposed design and that of [1] is shown in Table 2. As shown in Table 2, our design excels the ones given in [1] in the gain, while our design has less bandwidth at the resonance frequencies.

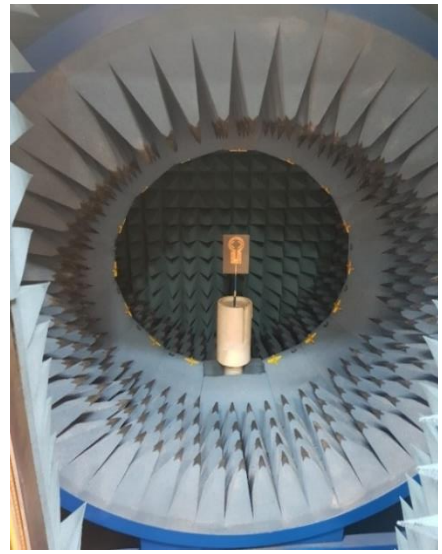

Fig. 9. Proposed antenna mounted in the Anechoic Chamber of the Military Excellence Center.

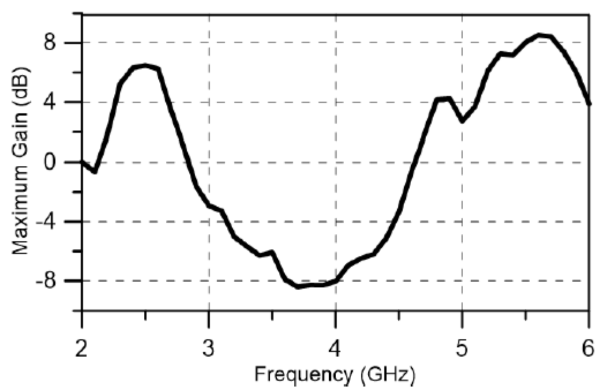

Fig. 10. Maximum gain versus frequency.

Table 2: Comparison between our results and [9]

	Resonance Frequency (GHz)	Bandwidth (MHz)	Maximum Gain (dB)
[9]	2.4	860	3.70
	5.8	590	7.57
Our Design	2.4	110	6.47 at $\phi = 92^0$, $\theta = -88^o$
	5.5	260	8.52 at $\phi = 142^0$, $\theta = -60^o$

The 3D total far electric field radiation pattern at 2.4 GHz produced from the simulation package is shown in Fig. 11.

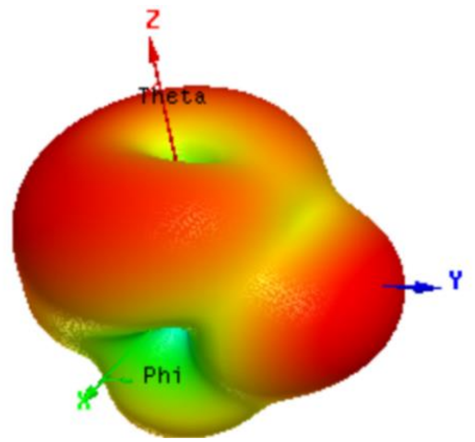

Fig. 11. 3D radiation pattern at 2.4GHz.

Therefore, the maximum radiation occurs in the upper half of the *x-y* plane. Accordingly, the antenna can radiate effectively along positive z-axis. In addition, there is a quite large lobe along the negative z-direction. The measured and simulated total far electric field radiation patterns in the *x-z* plane is shown in Fig. 12. An excellent agreement between the radiation patterns corresponding to the measured and the simulation results is observed.

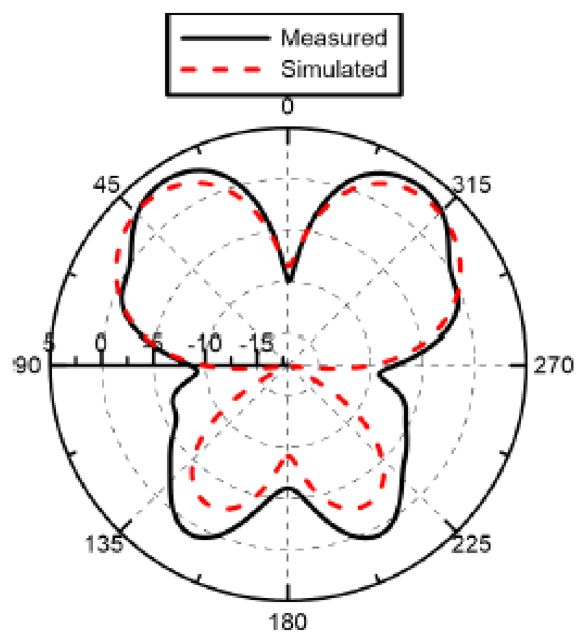

Fig. 12. Radiation pattern in the *x-z* plane at 2.4 GHz.

Other two-dimensional patterns in the *y-z* plane were calculated using the simulation package and compared with the corresponding measured pattern illustrated in Fig. 13. A reasonable agreement was found between the simulation and the measured patterns in this case.

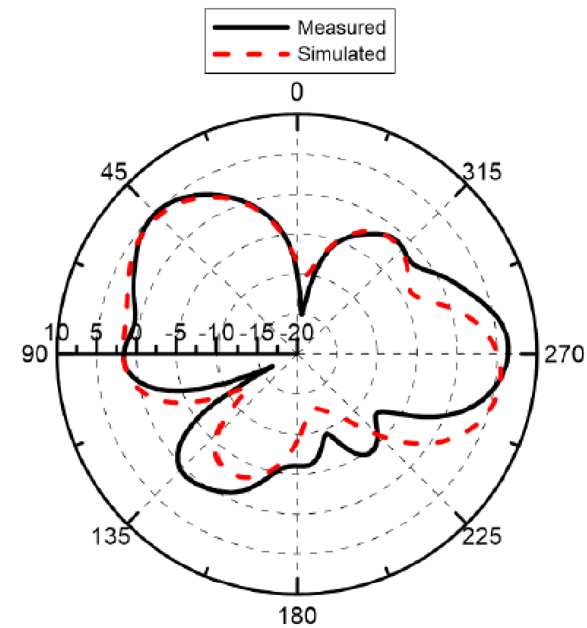

Fig. 13. Radiation pattern in the *y-z* plane at 2.4 GHz.

The 3D total far electric field radiation pattern at 5.5 GHz is illustrated in Fig. 14, while the radiation pattern in the *x-z* plane is shown in Fig. 15. A good agreement was found between simulation and measured patterns in this case. The perpendicular two-dimensional pattern in the *y-z* plane is obtained from the simulation package and compared with the corresponding measured pattern as shown in Fig. 16. A reasonable agreement was found between the simulation and the measured patterns in this case.

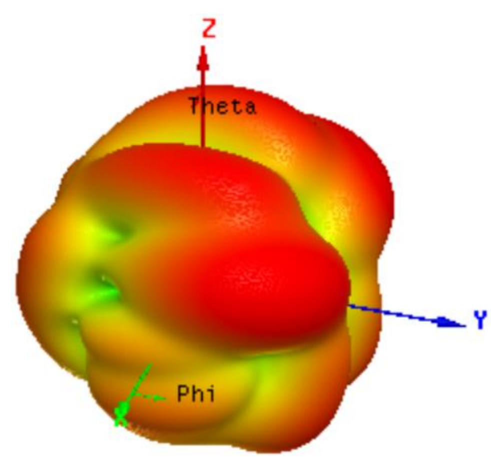

Fig. 14. 3D radiation pattern at 5.5 GHz.

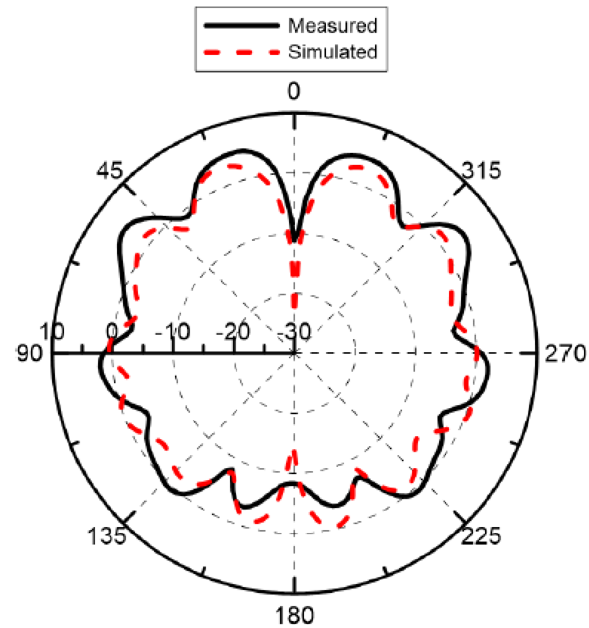

Fig. 15. *x-z* 2D radiation pattern at 5.5 GHz.

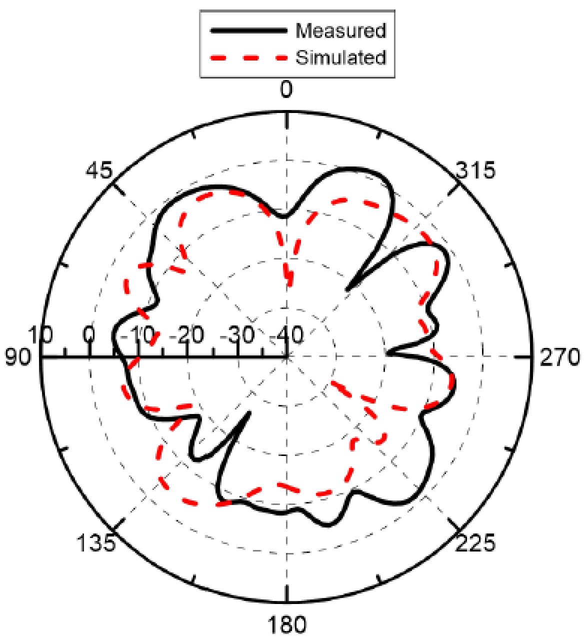

Fig. 16. y-z 2D radiation pattern at 5.5 GHz.

IV. CONCLUSION

A high gain dual-band microstrip patch antenna resonates at 2.4 GHz and 5.5 GHz for WI-FI, WIMAX and radio frequency identification reader application is successfully designed. The antenna is fabricated and tested where excellent agreement between theoretical and practical results is found. In addition, the maximum gain at 2.4 GHZ is about 6.47 dB while at 5.5 GHz is 8.52 dB. The proposed antenna has a simple configuration and it is easy to be fabricated. Experimental results excel the corresponding theoretical ones.

ACKNOWLEDGMENT

The author wishes to thank **The British University in Egypt** for providing all the facilities required to perform this research. Also, special thanks are due to Dr. Hani Ghali for supplying the antenna substrate.

REFERENCES

[1] O. Amjad, S. W. Munir, S. T. İmeci, and A. Ö. Ercan**,** "Design and implementation of dual band microstrip patch antenna for WLAN energy harvesting system," *Applied Computational Electromagnetics Society Journal*, vol. 33, no. 7, pp. 746-751, July 2018.

[2] E. K. I. Hamad, "Design and implementation of dual-band microstrip antennas for RFID reader application," *Ciência e Técnica Vitivinícola*, vol. 29, no. 9, pp. 2-10, Sep. 2014.

[3] M. R. Ahsan, M. T. Islam, M. H. Ullah, H. Arshad, and M. F. Mansor, "Low-cost dielectric substrate for designing low profile multiband monopole microstrip antenna," *The Scientific World Journal*, vol. 2014, Article ID 183741, 10 pages. http://dx.doi.org/10.1155/2014/183741

[4] S. Heydari, K. Pedram, Z. Ahmed, and F. B. Zarrab, "Dual band monopole antenna based on metamaterial structure with narrowband and UWB resonances with reconfigurable quality," *International Journal of Electronics and Communication (AEÜ)*, vol. 81, pp. 92-98, 2017.

[5] I. Md Rafiqul, A. A. A. Alsaleh, M. Aminah W. N., M. S. Yasmin, and N. Farihah A. M., "Design of dual band microstrip patch antenna using metamaterial," *6th International Conference on Mechatronics - ICOM'17*, 2017. doi:10.1088/1757-899X/260/1/012037.

[6] S. X. Ta and I. Park, "Dual-band operation of a circularly polarized four-arm curl antenna with asymmetric arm length," *International Journal of Antennas and Propagation*, vol. 2016, Article ID 3531089, 10 pages, 2016.

[7] I. Ali and R. Y. Chang, "Design of dual-band microstrip patch antenna with defected ground plane for modern wireless applications," *2015 IEEE 82nd Vehicular Technology Conference (VTC2015 Fall)*, 2015.

[8] N. H. Gad and M. Vidmar**,** "Design of a microstrip-fed printed-slot antenna using defected ground structures for multiband applications," *Applied Computational Electromagnetics Society Journal*, vol. 33, no. 8, pp. 854-860, Aug. 2018.

[9] J. R. Panda and R. S. Kshetrimayum, "A printed 2.4 GHz/5.8GHz dual-band monoploe antenna with a protruding stub in the ground plane for

WLAN and RFID applications," *Progress in Electromagnetics Research (PIER)*, vol. 117, pp. 425-434, 2011.
[10] N. Angkawisittpan and Apirat Siritaratiwat, "A dual frequency monopole antenna with double spurlines for PCS and Bluetooth applications," *Applied Computational Electromagnetics Society Journal*, vol. 31, no. 8, pp. 976-981, Aug. 2016.
[11] M. Ojaroudi, N. Ojaroudi, and N, Ghadimi, "Enhanced bandwidth small square slot antenna with circular polarization characteristics for WLAN/ WiMAX and C-band applications," *Applied Computational Electromagnetics Society Journal*, vol. 28, no. 2, pp. 156-161, Feb. 2013.
[12] M. Rafaei-Booket and A. Jafargholi, "Dual-Band compact array of printed dipole antennas," *Applied Computational Electromagnetics Society Journal*, vol. 30, no. 3, pp. 319-326, Mar. 2015.
[13] C. Balanis, *Antenna Theory*. 2nd edition: Wiley, 1997.
[14] D. Pozar, *Microwave Engineering*. 2nd edition: Wiley, 1998.

Hassan Ragheb was born in Port-Said, Egypt, in 1953. He received the B.Sc. degree in Electrical Engineering from Cairo University, Egypt, in 1977, and the M.Sc. and Ph.D. degrees in Electrical Engineering from the University of Manitoba, Winnipeg, Canada, in 1984 and 1987, respectively. From 1987 to 1989, he was a Research Assistant at the Department of Electrical Engineering, University of Manitoba. From 1989 to 2016, he was with the Department of Electrical Engineering at the King Fahd University of Petroleum and Minerals, Saudi Arabia, where he was a Professor of Electrical Engineering. In January 2018, he joined the Electrical Engineering Department at the British University in Egypt where he is currently a Professor of Electrical Engineering. His research interests include electromagnetic scattering by multiple and coated objects, microstrip antennas, phased arrays, slot and open ended waveguide antennas.

Shady Nagaty was born in Cairo, Egypt, September 1996. He received the B.Sc. degree in Electrical and Communication Engineering from The British University in Egypt (BUE) in 2019. He has an Embedded System Diploma granted by the Egyptian Engineers Syndicate (2016). He attended an internship program at the National Center for Energy Control (2017). He also succeeded to obtain an internship in Huawei corporate.

Afaf Saad was born in Makkah, Saudi Arabia, in 1992. She received her B.Sc. degree in Electrical and Communication Engineering from The British University in Egypt, with a grade of "Distinction with Honors," 2014. Currently, she is a Teaching Assistant at the Electrical and Communication Engineering Department at the British University in Egypt. She now finalizes her Master's thesis in "Early Detection of Masses in Digitized Mammograms".

Ahmed Zaalouk was born in 1994 in Cairo, Egypt. He is a fresh graduate engineer who has obtained his BA from the British University in Egypt (BUE) with a grade of Distinction with Honors, 2018. Zaalouk is currently enrolled in a Master's degree program in Computer Engineering at Ain Shams University.